Liquid-crystal–solid interface structure at the antiferroelectric-ferroelectric phase transition

D. Coleman, S. Bardon, L. Radzihovsky, G. Danner, and N. A. Clark
Condensed Matter Laboratory, Department of Physics, University of Colorado, Boulder, Colorado 80309
(Received 13 June 2002; published 30 December 2002)

Total internal reflection is used to probe the molecular organization at the surface of a tilted chiral smectic liquid crystal at temperatures in the vicinity of the bulk antiferroelectric-ferroelectric phase transition. Data are interpreted using an exact analytical solution of a real model for ferroelectric order at the surface. In the mixture *T*3, ferroelectric surface order is expelled with the bulk ferroelectric-antiferroelectric transition. The conditions for ferroelectric order at the surface of an antiferroelectric bulk are presented.

DOI: 10.1103/PhysRevE.66.061709 PACS number(s): 61.30.Eb

Antiferroelectric and antiferromagnetic ordering occurs when there is a sufficiently strong local interaction favoring antiparallel neighboring dipoles or spins. The result is macroscopic ordering that is nonpolar in the absence of external fields. By contrast, material surfaces are inherently polar, there being an obvious direction from one material to another. Therefore at the surface of antiferroelectrics, there is an intrinsic competition between the bulk antiferroelectricity and the surface ferroelectric ordering tendency. Liquid crystals (LCs) are an attractive system for studying this behavior because their large optical anisotropy and sensitivity to surface forces make effective study of surface states possible. In this paper, we investigate surface structure of tilted chiral smectic LCs, two-dimensional polar fluid layers of rod-shaped molecules that order into either ferroelectric or antiferroelectric bulk structures.

In a given tilted smectic liquid-crystal layer, $\hat{n}$, the orientation of the mean long molecular axis is given by θ, the fixed angle of tilt relative to the layer normal $\hat{z}$, as shown in Fig. 1, and by $\phi(x)$, the azimuthal orientation about $\hat{z}$, a Goldstone variable degenerate in the free energy in an infinite sample. Chiral tilted smectic layers are ferroelectric, the lack of mirror symmetry allowing within each layer a spontaneous polarization **P** mutually perpendicular to $\hat{n}$ and $\hat{z}$ (see Fig. 1). This enables coupling of ϕ to electric field **E** applied in the plane of the layer, tending to minimize $\mathbf{P}\cdot\mathbf{E}$. In the synclinic ferroelectric (SYN, Sm-C^*) tilted chiral smectic phase [1], adjacent layers are tilted in the same direction ($\Delta\phi=0$), whereas, in the Anticlinic Antiferroelectric (ANTI, Sm-C_A^*) phase [2], adjacent layers are tilted in opposite directions ($\Delta\phi=\pi$).

We consider here LC-solid surface systems wherein the molecules at the surface prefer (planar) alignment, i.e., with $\hat{n}$ parallel to the substrate plane. In a Sm-C^* with the layers oriented perpendicular to the substrates (bookshelf geometry) and with the helix unwound (i.e., surface stabilized [3]), such planar alignment will generate *two* preferred $\hat{n}$ orientations corresponding to the intersection of the tilt cone with the substrate [$\phi(0)=0$ and $\phi(0)=\pi$ in Fig. 1]. Additionally, LC chirality couples with the polar nature of the surface to produce a surface energy difference $\Delta U_{\mathrm{Surf}}=U_{\mathrm{Surf}}(0)-U_{\mathrm{Surf}}(\pi)$ between these two states, tending to produce a uniform synclinic order at the surface. By contrast, in the Sm-C_A^* bookshelf geometry, the bulk anticlinic ordering is basically incompatible with the synclinic order preferred by the surface. A strong polar surface interaction will cause the system to minimize its energy by adopting synclinic order near the surface, lowering the surface energy at the expense of increasing that of the anticlinic bulk [Fig. 1(b)]. With sufficiently small ΔU_{Surf}, the ferroelectric order at the surface may be expelled by the antiferroelectric bulk. The geometry will then be the configuration of Fig. 1(a) in which the LC is uniformly anticlinic with $\phi(0)$ equal to 0 and π in adjacent layers, and having planar alignment of $\hat{n}$. We have carried out total internal reflection (TIR) measurement of the optic axis director orientation in the LC-solid interface in bookshelf tilted chiral smectic cells with planar aligned surfaces [4,5]. This technique enables us to readily distinguish syn-

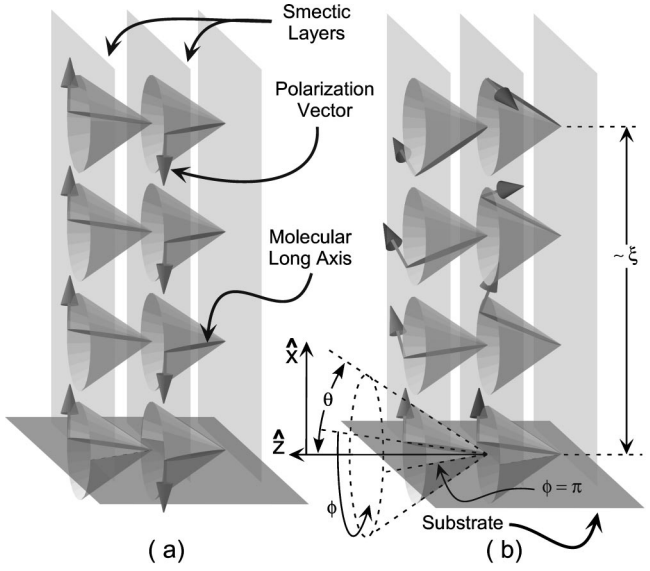

FIG. 1. (a) Schematic of the director and polarization profiles for the uniform anticlinic tilted chiral smectic with boundary surfaces perpendicular to the smectic layers. We assume that the dominant surface interaction energy is the planar interaction favoring molecular alignment along the surface. (b) The model for a synclinic distortion at the surface of an anticlinic bulk smectic material. The polar nature of the surface favors a certain sign of polarization in competition with the bulk antiferroelectricity. In the model for the distorted state, the polarization makes an angle ϕ with the surface normal and the distortion has a penetration depth ξ.

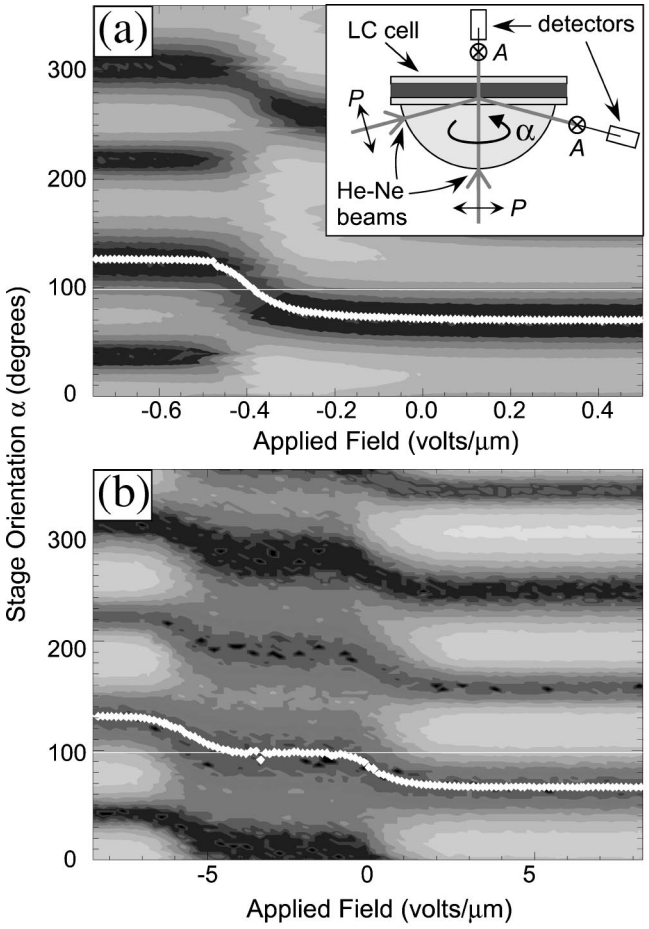

FIG. 2. Contour plot of the depolarized intensity of the TIR signal vs applied voltage and stage angle in the SYN (a) and ANTI (b) phases as a function of voltage. The layer normal is indicated by the horizontal solid line and the orientation of the optical axis, β, is indicated by the open diamonds. Inset: Setup for the TIR study of the LC orientation near the glass surface via depolarization of the reflected He-Ne beam. The beam incident along the hemisphere axis probes the orientation of the optical axis of the bulk LC.

clinic surface and anticlinic surface states. The results are interpreted using an exact analytic solution of a realistic theoretical model of surface ordering.

The TIR setup is presented in the inset to Fig. 2. A He-Ne laser beam polarized in the plane of incidence illuminates the LC cell through a high refractive index hemisphere ($n=1.79$) at a fixed angle of incidence of 75°. The light is totally reflected at the glass-LC interface, and an evanescent wave (probe beam) penetrates a depth $\lambda \sim 1000$ Å into the LC. Hereafter, we will denote the depolarization ratio $R(\alpha)$ as the ratio of the detected *s*-wave (out of plane) intensity to the incident *p*-wave (in plane) intensity. $R(\alpha)$, measured as a function of α, the angle between $\hat{z}$ and the TIR plane of incidence, gives information about the orientation of the LC close to the TIR interface. Minima in $R(\alpha)$ occur when an optical axis is rotated to be either parallel or perpendicular to the TIR plane of incidence. That is, a uniform director along $\hat{z}$ produces four zero-intensity minima in $R(\alpha)$ at $\alpha=0,\pi/2,\pi,3\pi/2$. As the director tilts out of the $\hat{z}$-$\hat{y}$ plane by an angle γ [in a planar-aligned Sm-*C* cell, $\tan\gamma=\sin\theta\sin\phi(1-\sin^2\theta\sin^2\phi)^{-1/2}$] the director is no longer perpendicular to the plane of incidence at $\alpha=\pi/2,3\pi/2$. $R(\alpha=\pi/2,3\pi/2)$ becomes nonzero and grows rapidly with increasing γ, evolving continuously to become a global maxima for $\gamma>17°$ (for a material with average index of refraction, n_{avg}, equal to 1.58 and birefringence, Δn, equal to 0.1). We determined the orientation of the bulk optical axis of the LC by using an additional laser beam at normal incidence to the cell plates to probe the cell birefringence via measurement of the transmission $[T(\alpha)]$ between crossed polarizer and analyzer. $T(\alpha)=0$ corresponds to having a uniformly oriented optical axis that projects onto the *y*-*z* plane parallel to the polarizer or analyzer.

We performed experiments in the (SYN, Sm-C^*) and (ANTI, Sm-C_A^*) phases of the three component mixture, *T*3 [6,7], which has the phase sequence: Iso [69 °C] Sm-A^* [64 °C] Sm-C^* [43 °C] Sm-CA^*. The Sm-C^* phase can be expected to have SYN order at the surface and a phase transition to a bulk ANTI phase that may or may not be accompanied by a change in the surface ordering. The high index glass substrate at the TIR interface was coated with a 590-Å-thick transparent conducting indium tin oxide (ITO) layer ($n=1.96$) and then a 150-Å-thick rubbed nylon (Du Pont Elvamide 8023) alignment layer to produce uniform smectic layering. The glass-ITO-nylon-LC assembly produces a TIR condition only at the ITO-nylon interface. The other cell surface was coated with unrubbed nylon. The bulk optic axis reorientation saturates with $\hat{n}$ on opposite sides of the tilt cone, $\phi=(0,\pi)$ at ± 8 V/μm, respectively, enabling a determination of the layer normal from the average optic axis orientation and of the tilt angle θ, half the difference in the optic axis orientations. For *T*3, $\theta=31°$ in the Sm-C^* ($T=48$°C) and $\theta=36°$ in the Sm-C_A^* ($T=25$ °C). The *T*3 cells are surface stabilized.

Figure 2 shows contour plots of $R(\alpha)$ vs α and applied (decreasing) electric field **E** at 48 °C and 25 °C, well into the Sm-C^* and Sm-C_A^* phase ranges, respectively. In both phases there are four minima in $R(\alpha)$ at zero volts and at the positive and negative saturated voltages indicating that the average optic axis within 1000 Å of the surface is uniform and parallel to the surface. In the Sm-C^* phase at $\mathbf{E}=\mathbf{0}$ the optic axis at the surface is rotated by 27° from the layer normal, close to $\phi=0$ on the tilt cone and parallel to the surface. Application of $\mathbf{E}>\mathbf{0}$ produces little change, but application of $\mathbf{E}<\mathbf{0}$ above a threshold magnitude $|E| \approx 0.4$ V/μm favoring $\phi=\pi$ overcomes the polar surface pinning to stabilize $\phi=\pi$ at the surface and reorient the bulk Sm-C^*. During switching, the minima corresponding to the optical axis perpendicular to the plane of incidence disappear, indicating tilt relative to the surface as the molecules reorient on the smectic-*C* cone. By contrast, in the Sm-C_A^* phase, the surface optic axis is nearly along the bulk layer normal at $\mathbf{E}=\mathbf{0}$ and the maxima in $R(\alpha)$ are reduced because of the smaller birefringence of the antiferroelectric (AF) ordering at the surface. Application of either sign of **E** produces a thresholded transition to FE order at the surface that is observed simultaneously in the bulk Sm-C_A^*. Further-

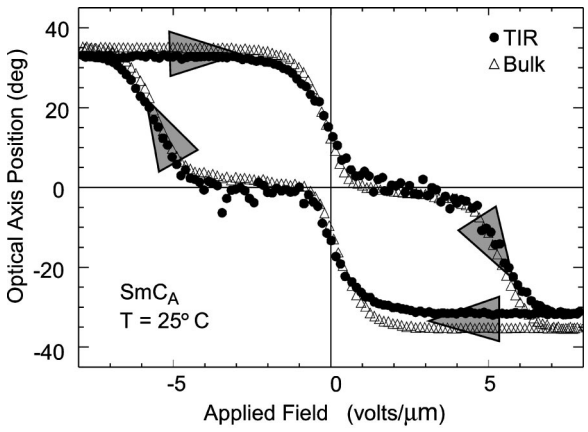

FIG. 3. Evolution of the optical axis relative to the layer normal (β) with applied field in the Sm-C_A^* phase. The bulk signal displays the expected three state switching with large hysteresis. The surface orientation follows the bulk to within 4°.

more, all four minima of $R(\alpha)$ maintain roughly equal intensity throughout the switching indicating that there is never any tilt of the optic axis at the surface in the AF phase.

In Fig. 3, we present the evolution of the orientation, β, of the optical axis relative to the layer normal in the surface and bulk at 25 °C in the Sm-C_A^* phase for a voltage ramp from -9 to $+9$ V/μm at 0.5 mHz. In response to this ramp, the bulk and surface orientations both exhibit a hysteretic transition between AF and FE states. For both positive and negative voltages, the surface saturates to a smaller angle than the bulk ($|\beta_{\rm surf}|<|\beta_{\rm bulk}|$). In the surface-preferred positive voltage state, the surface saturates to a tilt angle of 32°, 4° less than the bulk. However, in the surface disfavored negative voltage state, the surface saturates to a tilt angle of 34°, only 2° less than the bulk. Upon $\mathbf{E}\rightarrow 0$, the surface optical axis orientation does not return completely to be along the layer normal, indicating some kind of remnant FE order characteristic of the state that it was previously in. The small remnant angle ($\sim 2°$) could be accounted for by a weakly polar state having $\mathcal{P}$ at the surface rotated a few degrees from the ANTI state. A 40-Å-thick strongly FE remnant layer (i.e., with $\phi=\pi$) could also produce such a rotation. $R(\alpha)$ data such as in Fig. 2 were measured vs temperature near $T=T_{\rm SA}$ (the ANTI to SYN phase transition temperature), where, because of the ambivalence of the bulk ordering, one might expect SYN surfaces with ANTI bulk. However, measured bulk and surface optic axis orientations show a similar temperature dependence and indicate that if the state with SYN surfaces and ANTI bulk occurs, it is only over a small temperature range near $T_{\rm SA}$ ($T_{\rm SA}-T<1.8$ °C).

Further interpretation of this temperature behavior requires a calculation of the structure of $\phi(x)$ using a quantitative model of the bulk and surface energetics. We model the ϕ dependence of the surface energy per unit area by

$$U_{\rm Surf}=-S_p\cos\phi-S_{np}\cos 2\phi, \tag{1}$$

having polar (S_p) and nonpolar (S_{np}) interaction coefficients. We model the ϕ dependence of the bulk energy per unit volume by nearest neighbor layer interactions of the form

$$U_{\rm Bulk}=U_p[1+\cos(\phi_\ell-\phi_{\ell+1})]+U_{np}[1-\cos 2(\phi_\ell-\phi_{\ell+1})], \tag{2}$$

with U_p and U_{np} chosen so that $U_{\rm Bulk}$ exhibits a local minimum for the SYN orientation and a global minimum for the ANTI orientation; $2U_p$ is the energy difference between the ANTI and SYN states in the absence of a surface, while $U_B=(U_p+4U_{np})^2/8U_{np}$ is the height of the energy barrier between these states.

To model the surface order in the ANTI phase, two configurations shown in Figs. 1(a) and 1(b) need to be considered. The uniform configuration is an ANTI state right down to the surface that minimizes the bulk energy and the nonpolar surface energy while the polar surface energy alternates between the stable and unstable minimum values ($U_{\rm Surf}=-S_{np}-S_p$ and $U_{\rm Surf}=-S_{np}+S_p$ in adjacent layers). The bulk energy of the Uniform configuration is zero, $U_{\rm Bulk}=0$, with a total energy $E_U=-LNdS_{np}$ where L is the cell length, N is the number of layers in the cell, and d is the layer thickness. Both configurations have an average optic axis in the $\hat{z}$-$\hat{y}$ plane, thus satisfying the zero-pretilt required by the four minima in $R(\alpha)$ [Fig. 1(b)].

In the distorted configuration, a bulk ANTI state deforms into a SYN state at the surface, where in general $\phi(0)\neq 0$. We assume that the $\phi_l(x)$ for all even layers are identical and the negative of their odd neighbors, i.e., $\phi_\ell(x)=-\phi_{\ell+1}(x)$, reducing the problem to the determination of the single field, $\phi(x)$, degree of freedom. Working in the one-elastic constant approximation, the bulk free energy arising from elastic deformation, layer-layer interaction, and polarization self-interaction is given by

$$H_b[\phi(x)]=A\int_0^\infty dx\left[\frac{1}{2}K\left(\frac{d\phi}{dx}\right)^2+U_{\rm Bulk}(\phi)+\frac{1}{2\epsilon_o}\mathcal{P}^2\cos^2(\phi)\right], \tag{3}$$

where $A=LNd$. The form of the polarization self-interaction energy (the third term) [8] is the same as the polar term in the interlayer potential so that $U_p\rightarrow U_p+(\mathbf{P}^2/4\epsilon_o)$ in the following discussion. A solution, $\phi(x)$, minimizing the bulk energy $H_b[\phi(x)]$, subject to the constraint at the surface, $\phi(0)$, has a sigmoidal, solitonlike form characterized by a penetration length $\xi\approx\sqrt{K/(U_p+4U_{np})}$ and can be found exactly via standard methods. Inserting this solution $\phi(x)$ into Eq. (3), we find the bulk energy as a function of the surface polarization boundary condition, $\phi(0)$,

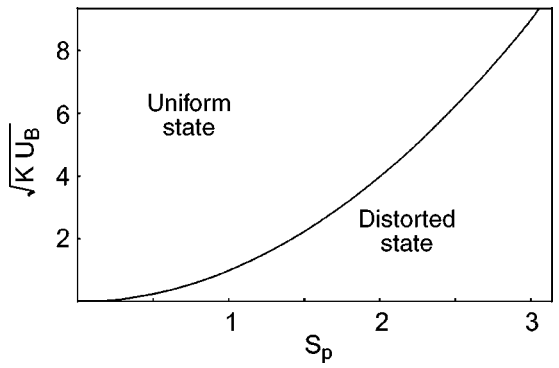

FIG. 4. Phase diagram for uniform and distorted states as a function of the polar surface potential (S_p) and the barrier between the synclinic [Fig. 1(b)] and anticlinic [Fig. 1(a)] states (U_B).

$$H_b[\phi(0)] = A\frac{\sqrt{K}}{2}\tan\phi(0)[U_p + U_{np} + U_p\cos 2\phi(0) - U_{np}\cos 4\phi(0)]^{1/2} - A\frac{U_p}{4}\sqrt{\frac{2K}{U_{np}}} \times \arctan\left(\frac{2\sqrt{\frac{U_{np}}{U_p}}\sin\phi(0)}{\sqrt{U_p + 2U_{np} - 2U_2\cos 2\phi(0)}}\right). \tag{4}$$

Combining this bulk energy with the energy of the surface [Eq. (1)], we can exactly find the energy of the distorted state and the equilibrium surface angle $\phi(0)$ by minimizing the total energy $E_D = H_b[\phi(0)] + AU_{\mathrm{Surf}}[\phi(0)]$ over $\phi(0)$.

The bulk Sm-C^* to Sm-C_A^* transition is first order as evidenced by coexistence of Sm-C^* to Sm-C_A^* domains in electro-optic experiments. Consequently, $U_B > 2U_p$ (where U_p includes the polarization self-interaction) so that U_B always provides the dominant contribution to the distortion energy. For the range of parameters relevant to our experiment, it can be shown that H_b is proportional to $\sqrt{KU_B}$. Because both the uniform and distorted states minimize the planar interaction energy in Eq. (1), S_{np} gives approximately equal contribution to the energy of both the uniform and distorted states. This leaves only $\sqrt{KU_B}$ and S_p as competing energies to determine the stability of the distorted state and leads to the phase boundary illustrated in Fig. 4. There is a critical value, $S_{pc} \propto \sqrt{KU_B}$, above which the polar surface interaction is strong enough to induce the ferroelectric distortion. For LC-surface systems where $\sqrt{KU_B} > S_p$, the surfaces are too weak to pay the energy cost of the ferroelectric distortion and the LC will be uniformly antiferroelectric with surface optic axis along the layer normal.

This analysis shows that it is essential to include the nonpolar term in the bulk free energy in calculations of surface states of AF LCs. Although with high $\mathcal{P}$ there is always a polar term in the free energy, this contribution will be unimportant in low $\mathcal{P}$ mixtures near the Sm-C^* to Sm-C_A^* transition, but the barrier between the synclinic and anticlinic states (provided by the nonpolar term) should still be present and will determine the surface state.

One possible explanation for the difference between the bulk and the surface optic axis orientation at zero applied field is a weakly ferroelectric surface state characterized by $\phi(x=0) \approx \pi/2$ and a long penetration depth into the bulk. However, our model demonstrates that FE surface states with large ϕ ($\mathcal{P}$ only slightly rotated from the AF orientation) are energetically unfavorable compared to the uniform state. Consequently, for a ferroelectric layer to explain a small optical axis rotation, the layer must have small $\phi(x=0)$ and small decay length. From measurements of the polarization ($P = 170$ nC/cm^2 [9]) and the critical field for inducing the ferroelectric state (5 V/μm), we deduced the value of parameter $U_1 = 8.5$ kJ/m$^3 \sim U_B$. We then used a typical value for a liquid-crystal elastic constant to estimate the decay length $\xi \approx 1000$ Å of the ferroelectric surface order in the T3-nylon system. This decay length is similar to the TIR probe depth so that a TIR measurement of a $T3$ cell in the distorted state will detect an optical axis oriented along the tilt cone. Consequently, according to this model, the $T3$-nylon system at 25°C is in the uniform state.

The discovery of a material with a second-order Sm-C^* to Sm-C_A^* phase transition and small polarization, $\mathcal{P}$, would present the opportunity to observe the distorted state as described by our model. As long as bulk energy dominates, $\sqrt{KU_B} > S_{pc}$ at $T = T_c$, the cell will remain in the uniform state until the bulk transition is reached. However, at a second-order phase transition, U_B vanishes as $T \to T_c^-$. At some finite temperature below the transition, $\sqrt{KU_B}$ would be less than S_p and the distortion would appear. Furthermore, as the LC approaches the second-order transition from below, the decay length diverges. This would have the effect of reducing the AF to FE transition temperature in thin cells, where the cell thickness is of order of the decay length.

We conclude that in systems with surface interactions strong enough to induce ferroelectricity, the ferroelectricity will extend into the bulk over a distance ξ governed by K and U_B. For a first-order Sm-C_A^* to Sm-C^* transition, the polar surface term must be larger than $\sqrt{KU_B}$ to induce the ferroelectric state. However, for second-order transition, the distorted state always appears below T_c. Consequences of this are a pretransitional ferroelectric ordering at the surface and the depression of T_c in thin cells. Based on our measurements, we conclude that the polar surface interactions are not strong enough to induce ferroelectric surfaces in the $T3$-nylon system. It may be possible to increase the polar surface interaction, perhaps by using a material with a larger surface electroclinic effect [10,11].

This work has been supported by NSF MRSEC Grant No. DMR-9809555 and AFOSR MURI Grant No. F49620-97-1-0014.

[1] R.B. Meyer, L. Liebert, L. Strzelecki, and P. Keller, J. Phys. (France) Lett. **36**, L69 (1975).
[2] A.D.L. Chandani, T. Hagiwara, Y. Ouchi, H. Takezoe, and A. Fukuda, Jpn. J. Appl. Phys., Part 1 **27**, L729 (1988).
[3] N.A. Clark and S.T. Lagerwall, Appl. Phys. Lett. **36**, 899 (1980).
[4] J. Xue, N.A. Clark, and M.R. Meadows, Appl. Phys. Lett. **53**, 2397 (1988).
[5] Z. Zhuang, N.A. Clark, and M.R. Meadows, Phys. Rev. A **45**, R6981 (1992).
[6] A. Fukuda, in *Proceedings of the 15th International Display Research Conference of the Society for Information Display, Asia Display, 1995* (Institute for Television Engineers of Japan and the Society for Information Display, Hammamatsu, Japan, 1995), p. 61; S. Inui, N. Iimura, T. Suzuki, H. Iwane, K. Miyachi, Y. Takanishi, and A. Fukuda, J. Mater. Chem. **6**, 671 (1996).
[7] S.S. Seomun, B. Park, A.D.L. Chandani, D.S. Hermann, Y. Takanishi, K. Ishikawa, H. Takezoe, and A. Fukuda, Jpn. J. Appl. Phys., Part 2 **37**, L691 (1998).
[8] Z. Zhuang, J.E. Maclennan, and N.A. Clark, Proc. SPIE **1080**, 110 (1989).
[9] P. Rudquist, J.P.F. Lagerwall, M. Buivydas, F. Gouda, S.T. Lagerwall, N.A. Clark, J.E. Maclennan, R. Shao, D.A. Coleman, S. Bardon, T. Bellini, D.R. Link, G. Natale, M.A. Glaser, D.M. Walba, M.D. Wand, and X.-H. Chen, J. Mater. Chem. **6**, 1257 (1999); The Sm-$C^{\star}$ phase in this material exhibits high contrast analog electro-optic response to an applied electric field, initially mistakenly identified as a ''thresholdless antiferroelectric'' random tilted chiral smectic.
[10] J. Xue and N.A. Clark, Phys. Rev. Lett. **64**, 307 (1990).
[11] R. Shao, J.E. Maclennan, N.A. Clark, D.J. Dyer, and D.M. Walba, Liq. Cryst. **28**, 117 (2001).